Evidence for rhombohedral boron nitride in cubic boron nitride films grown by ion-assisted deposition

D. L. Medlin, T. A. Friedmann,* P. B. Mirkarimi, M. J. Mills, and K. F. McCarty
Sandia National Laboratories, Livermore, California 94551
(Received 7 March 1994)

We present high-resolution transmission electron-microscopic observations of the sp^2-bonded material that remains with the sp^3-bonded cubic boron nitride (cBN) in films grown by ion-assisted deposition. These observations show regions of sp^2-bonded material that are in a three-layer stacking configuration rather than the two-layer configuration of hexagonal boron nitride. Measurement of the lattice fringe angles shows that the observed three-layer stacking is consistent with the metastable, rhombohedral structure (rBN). Significantly, rBN allows for a diffusionless pathway for cBN synthesis under high pressure, unlike the high-activation-energy route that is required to directly convert the hexagonal phase to cBN. This low-energy pathway is considered in relation to recent work in the literature indicating that ion-induced compressive stress plays a critical role in the synthesis of thin-film cBN.

The allotropes of boron nitride include two sp^2-bonded phases with hexagonal[1] and rhombohedral[2] structures (hBN and rBN) and two sp^3-bonded phases with cubic (zinc-blende)[3] and hexagonal (wurtzitic)[4] structures (cBN and wBN) (Fig. 1). Although cBN is synthesized in bulk form by conversion of hBN at high temperatures and pressures, low-pressure synthesis of cBN as a thin film is more difficult and succeeds only when the growing film is simultaneously irradiated with a high flux of ions, typically supplied either with an independent ion source or via a plasma and biased substrate. Only sp^2-bonded material, which generally has a disordered, turbostratic microstructure, will form in the absence of ion irradiation.[5]

The mechanistic role of the irradiation is not well understood, but recent work suggests that ion-induced film stress is important. Synthesis of cBN typically employs a mixture of nitrogen and inert gas ions at ion-atom arrival-rate ratios on the order of unity.[6] These conditions result in films possessing high residual compressive stresses (5–10 GPa).[7,8] Kester and Messier[6] have reported that the fraction of cBN in the films can be rationalized for a particular ion-gas composition in terms of a momentum-related parameter that scales as the square root of the ion energy. Below a certain threshold of this parameter, no cBN is formed. Similar scaling with ion energy (although with a different mass dependence) is reported by Mirkarimi *et al.*[9] It is significant that for a variety of materials the magnitude of the ion-induced film stress can also be parametrized with an $E^{1/2}$ dependence.[10] McKenzie *et al.*[8] note both a positive correlation between compressive film stress and cBN fraction as well as a threshold stress below which no cBN is detected. When resolved into its hydrostatic component, this threshold is comparable to the phase-stability boundary between cBN and hBN, extrapolated to low temperature (500 K). On the basis of these observations, McKenzie *et al.*[8] propose that the ion-assisted synthesis of cBN is induced by the high compressive stresses.

Although this explanation gives a thermodynamic justification for the formation of cBN in such films, questions remain regarding the pathway by which the transformation would proceed. McKenzie *et al.*[8] suggest that an ion-induced thermal spike locally melts a small volume of the film that then resolidifies, under pressure, to form cBN. It is worthwhile, however, to also consider the processes involved in a direct, solid-state transformation. Typically, BN films are deposited at temperatures less than 1000 °C, a regime for which the structure of the

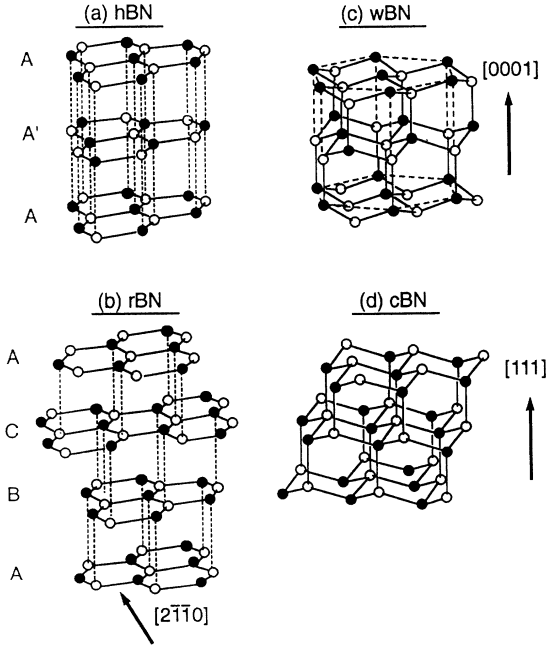

FIG. 1. Schematics of the hBN (a), rBN (b), wBN (c), and cBN (d) structures. Note the two-layer repeat sequence ($AA'AA'\cdots$) for hBN and the three-layer repeat sequence ($ABC\cdots$) for rBN and the similarity with, respectively, wBN and cBN. The optimum orientation for imaging the stacking sequences in rBN and hBN using HRTEM is along a $\langle 2\bar{1}\,\bar{1}0\rangle$ direction.

sp^2-bonded precursor material dictates the phase and microstructure of the material that forms from conventional (bulk) high-pressure treatment.[11,12] If the transformation in the thin-film case is also pressure induced, similar relationships should hold.

At present, however, little is known regarding the structure of the sp^2-bonded material that forms with the cBN in such films. Within unirradiated films (which have no cBN) the sp^2-bonded material is turbostratic, consisting of a random stacking of severely distorted, two-dimensional hexagonal networks. Ion irradiation during deposition increases the order of the sp^2-bonded material such that the basal (00l) planes grow in a highly oriented manner perpendicular to the substrate plane.[13] It has been thought that this more ordered sp^2-bonded material is in the hexagonal configuration. Interestingly, in recent x-ray absorption studies of similar films, Chaiken *et al.*[14] find near-edge features similar to those observed from bulk rBN powder. These authors note, however, that several possible causes for the features exist and that attribution of the effect to the presence of rBN is not definitive.

High-resolution transmission electron microscopy (HRTEM) provides a useful tool for investigating the local structure of the sp^2-bonded material. hBN and rBN differ in the stacking sequences of the planar hexagonal networks that form the layers of these structures. In hBN [Fig. 1(a)], these networks of six-membered $(BN)_3$ rings are aligned with no shear displacement between the layers. However, every other layer is rotated by 180° such that in the [0001] direction the positions of the boron and nitrogen atoms alternate in a two-layer stacking sequence. In rBN [Fig. 1(b)], all layers have the same rotation sense, but are successively displaced relative to the unsheared configuration by a vector of type $(a/3)\langle 01\bar{1}0\rangle$, resulting in a three-layer stacking sequence. Figure 2 shows high-resolution image simulations for hBN and rBN crystals oriented along a $\langle 2\bar{1}\,\bar{1}0\rangle$ direction (where both crystals are referenced to the hexagonal indexing system). For a large range of conditions there is sufficient contrast from the periodicities *within* the basal planes that the stacking sequences of the two structures can be distinguished.

Figure 3 shows a plan-view micrograph, obtained using a JEOL 4000EX HRTEM, from a boron nitride film grown at 800 °C by pulsed-laser deposition with 1-keV argon and nitrogen irradiation. Details regarding the deposition process and specimen preparation procedures are noted elsewhere.[5,15] The dominant fringes in this image correspond to the basal planes of the sp^2-bonded material, which exhibit a large degree of curvature. Specific areas (indicated by arrows) are sufficiently well aligned with a $\langle 2\bar{1}\,\bar{1}0\rangle$ direction that it is possible to observe the periodicities within the basal planes. A higher magnification view of the region indicated by the right arrow is shown in Fig. 4. The cross fringes in this region are not orthogonal to the basal fringes, and thus the material is not locally in the hBN configuration. Instead, the stacking of the fringes is consistent with the three-layer arrangement of the rhombohedral phase. Angles between sets of fringes (indicated in Fig. 4) were measured from the image and from the power spectrum of the image (see inset). As noted in Fig. 4, these angles compare well with those for the rBN structure. However, the three-layer arrangement has a limited spatial extent; the fringes near the bottom of the figure deviate to a configuration that is closer to hBN.

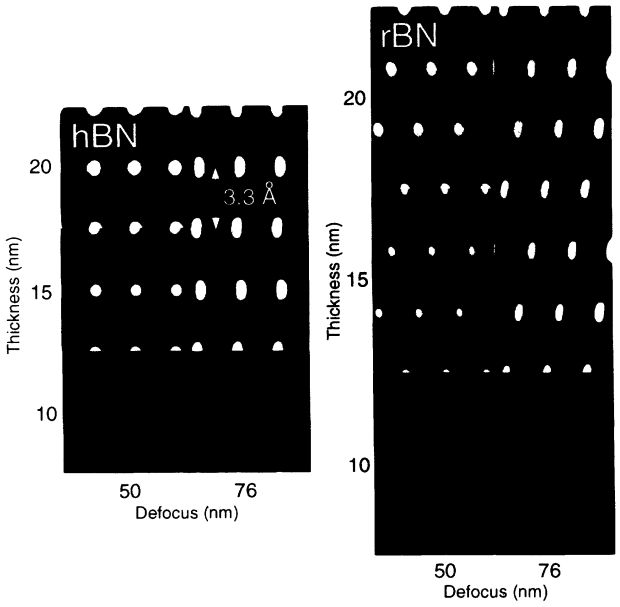

FIG. 2. High-resolution image simulations calculated as a function of thickness and defocus for hBN and rBN oriented along a $\langle 2\bar{1}\,\bar{1}0\rangle$ direction for the following conditions: electron energy, 400 keV; coefficient of spherical aberration, 1.0 mm; semiconvergence angle, 1.3 mrad; objective aperture diameter, 20 nm^{-1}; and spread of focus, 10 nm. Simulations calculated using the EMS package of electron microscopy routines (Ref. 28).

These observations are not conclusive proof that the sheared domains are in the rBN configuration. Specifically, we have not ascertained the rotation sense of the hexagonal networks. Although it is not possible to resolve the individual nitrogen and boron columns (which are separated by only 0.72 Å in a $\langle 2\bar{1}\,\bar{1}0\rangle$ projection), the different scattering for boron and nitrogen results in an intensity distribution that is asymmetric (see Fig. 2).

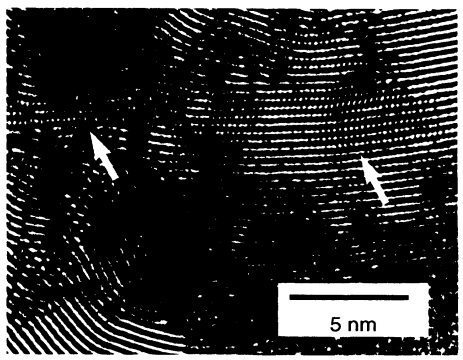

FIG. 3. HRTEM image of turbostratic BN in a film deposited by ion-assisted pulsed-laser deposition. Defocus is 70 nm.

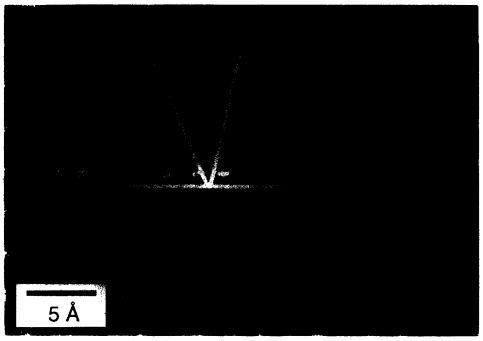

FIG. 4. Enlargement of region indicated by the rightmost arrow in Fig. 3. Angles measured from micrograph are as follows: (0003), $(01\bar{1}\,\bar{1})$, 66±2° (direct), 63±1° (power spectrum) and (0003), $(01\bar{1}2)$, 78±1° (direct), 78±1° (power spectrum). Calculated angles for rBN are as follows: (0003), $(01\bar{1}\,\bar{1})$, 66.5° and (0003), $(01\bar{1}2)$, 77.8°.

From the orientation of these dots it is possible, in principle, to identify the rotation sense of the particular basal plane (i.e., the intensity distribution reverses by 180° on alternate fringes in hBN but maintains a constant orientation in rBN), but the effect is weak and is strongly affected by deviations from perfect crystal tilt. Bending of the basal planes leads to large variations in tilt over a small spatial scale and such deviations can affect the image contrast and character.[16] We have simulated the effects of various combinations of crystal tilt (rotations of up to 30 mrad about the [0001] and $[01\bar{1}0]$ axes) from the $\langle 2\bar{1}\,\bar{1}0\rangle$ zones for both hBN and rBN. Although the relative shears of the hexagonal nets remain distinguishable over the investigated range of tilts, we note that the image contrast is significantly reduced, and in many cases the shape and local symmetry of the dots of contrast are sufficiently distorted to obscure the subtle asymmetry that arises from the alternating boron and nitrogen atoms.

Although we have not determined the rotation sense of the hexagonal networks, the observed three-layer stacking and measured fringe angles are strongly supportive of the formation of rhombohedrally configured sp^2-bonded material. This result is significant because rBN allows for the formation of cBN by a direct, diffusionless transformation that is an easier route than the high activation energy, reconstructive process that would be required to directly convert the hexagonal phase. Aside from the puckering, the stacking of the hBN (0002) and rBN (0003) planes is identical, respectively, to that of the wBN (0002) and cBN $\{111\}$ planes (see Fig. 1). These structural similarities determine the transformation pathway followed during low-temperature bulk compression. *Ab initio* simulations of the compression of hBN and rBN show a buckling of the networks followed by the change from sp^2 to sp^3 hybridization as these transform, respectively, to wBN and cBN.[17] These calculations suggest that the activation energy for the rBN to cBN pathway is less than 0.5 eV/atom, which is much smaller than the 4-eV/atom barrier[11] for the hBN-to-cBN pathway.

This direct mechanism is experimentally well established for both the hBN to wBN and the rBN to cBN transformations. Studies involving both static compression and shock loading of well-crystallized hBN at low temperature[11] show that the resulting material is predominantly wBN. This material is textured such that the hBN (0002) planes are parallel with the wBN (0002) planes.[18] At room temperature, the threshold pressure to induce this direct transformation is about 11 GPa,[4,19] and this drops to about 7 GPa at 1000 °C.[19] The pressure-temperature thresholds are not as well determined for the rBN to cBN transformation. Sato, Ishii, and Setaka[20] performed shock-loading experiments on hBN and rBN at pressures in excess of 40 GPa. Under identical conditions, hBN transformed to wBN whereas rBN transformed to cBN. Interestingly, in subsequent work by this group, wBN also formed from rBN shocked at pressures between 17 and 40 GPA,[21] which indicates that alternative pathways exist for the transformation from rBN. Although the fraction of cBN in this study[21] is unclear because of the overlap of the cBN $\{111\}$ and wBN (0002) x-ray diffraction peaks, the relative intensity of this composite peak, compared with that of the wBN $\{10\bar{1}0\}$ and $\{10\bar{1}1\}$, suggests that cBN was also present in appreciable quantities. Onodera *et al.*[22] performed low-temperature static-compression studies on rBN noting also the formation of both cBN and wBN. In a more recent study, however, this group observed that only cBN formed (starting at 8 GPa) during static compression of rBN at room temperature.[23] Earlier observations of wBN formation were attributed to deformation of the sp^2-bonded material from the original rBN configuration. Britun, Kurdyumov, and Petrusha[24] have proposed a twinning mechanism by which rBN deforms into an intermediate configuration that could lead directly to wBN. Thus, depending on the local stress distribution during the initial stages of the compression, rBN will transform either indirectly to wBN or directly to cBN. wBN can be distinguished from cBN on the basis of both diffraction and infrared absorption,[25] and the predominant sp^3-bonded phase in BN films grown with ion-beam assistance is the cubic phase. If the direct, solid-state transformation is occurring in the thin-film synthesis, then the rhombohedrally configured domains are likely to play a critical role.

The solid-state transformation will occur only if sufficient compressive stress is generated during the ion-assisted deposition. McKenzie *et al.*[8] note that cBN is formed only in films with residual biaxial stresses in excess of about 4 GPa, which resolved into its hydrostatic component corresponds to a pressure of 2.7 GPa. Although this pressure is above the equilibrium line between cBN and hBN (extrapolated from high temperatures), it is significantly less than even the lowest pressures for which direct bulk transformations have been observed. However, the *residual* film stress is necessarily less than the localized stress that exists during the irradiation. Compressive stress in films grown under a high-ion fluence is caused by the volumetric strain due to the implantation of ions and the formation of defects as the ion penetrates into the material. During the irradiation, the defect concentration is determined by the dynamic

balance between the defect-formation and recombination rates. A recent analysis of the variation of cBN concentration in films deposited over a range of ion masses and energies[9] indicates that such recombination must be considered in order to explain the observed energy and mass scaling. An important result from this work is that the scaling is controlled by the maximum in the depth distribution of the defect-formation rates and not by the absolute number of atomic displacements.

The implication of this result is that the distribution of stress within the growing film is neither uniform nor constant. Rather, the instantaneous volumetric strain is a maximum within the depth that ions penetrate into the film, but as the film thickens recombination of defects beyond the penetration depth reduces the stress. Therefore, even an *in situ* measurement will underestimate the peak stress since the measurement averages over the entire film thickness. The magnitude of this stress depends sensitively on the defect-formation and recombination rates and is difficult to estimate without a detailed understanding of the ion-solid interaction and the properties of the radiation-induced point defects. Nevertheless, considering the already large residual stresses, it is conceivable that the peak stresses exceed the pressure thresholds necessary to induce the transformation.

Under this compressive stress, then, the sp^2-bonded material would transform locally to the sp^3-bonded phase of closest structural similarity. Interesting, however, is the absence of the wurtzitic phase. One possibility is that both cBN and wBN form initially from separate rBN- and hBN-configured domains, but that the resulting cBN nuclei grow at the expense of the wBN by either a diffusive or shear process. Although the large activation energy for the wBN to cBN transformation [~4 eV/atom (Ref. 11)] prevents a diffusive transformation at reasonable rates for bulk static compression at temperatures below 1200 °C–1500 °C,[11,19] the high-defect concentrations that exist during ion-assisted deposition would be likely to enhance the rate. Conversion of the wBN to cBN via a nondiffusional shear process, as occurs when wBN is shock loaded,[18,26] would depend on the stress distribution during the deposition. A second possibility, however, is that most of the sp^2-bonded material forms initially in or near the rBN configuration and thereby can transform directly to cBN. Microstructural observations show that cBN thin films consist of crystallites with a high density of twin lamellae.[15,27] In this latter view, these defects simply reflect errors in the original stacking of the sp^2-bonded material. Further progress in addressing these issues would benefit from a quantitative assessment of the relative fractions of hBN and rBN in these films.

In summary, we have presented evidence for the presence of rhombohedrally configured boron nitride within the sp^2-bonded material that remains with cBN in films grown by ion-assisted deposition. Because of the structural similarities of the two phases, formation of rBN would provide a low-energy pathway to the cubic structure that is likely to be important in the stress-induced synthesis of thin-film cBN.

This research was supported by the U.S. DOE-OBES-DMS, under Contract No. DE-AC04-94AL85000. The authors thank W. G. Wolfer and J. E. Angelo for helpful discussions.

---

*Present address: Sandia National Laboratories, Albuquerque, NM 87185.

[1]R. S. Pease, Acta Crystallogr. **5**, 356 (1952).
[2]T. Ishii *et al.*, J. Cryst. Growth **52**, 285 (1981).
[3]J. R. H. Wentorf, J. Chem. Phys. **26**, 956 (1957).
[4]F. P. Bundy and R. H. Wentorf, J. Chem. Phys. **38**, 1144 (1963).
[5]T. A. Friedmann *et al.*, J. Appl.Phys. (to be published).
[6]D. J. Kester and R. Messier, J. Appl. Phys. **72**, 504 (1992).
[7]M. Okamoto, Y. Utsumi, and Y. Osaka, Plasma Sources Sci. Technol. **2**, 1 (1993).
[8]D. R. McKenzie *et al.*, Diamond Relat. Mater. **2**, 970 (1993).
[9]P. Mirkarimi *et al.*, J. Mater. Res. (to be published).
[10]H. Windischmann, Crit. Rev. Solid State Mater. Sci. **17**, 547 (1992).
[11]F. R. Corrigan and F. P. Bundy, J. Chem. Phys. **63**, 3812 (1975).
[12]A. V. Kurdyumov *et al.*, Izv. Akad. Nauk SSR, Neorg. Mater. **18**, 1835 (1983) [Inorganic Mater. (USSR) **18**, 1576 (1983)].
[13]D. K. Kester *et al.*, J. Mater. Res. **8**, 1213 (1993).
[14]A. Chaiken *et al.*, in *Covalent Ceramics II: Non-Oxides,* Proceedings of the Fall 1993 Meeting of the Materials Research Society, Symposium N, edited by A. R. Barron, G. S. Fischman, M. A. Fury, and A. F. Hepp (MRS, Pittsburgh, PA, 1994).
[15]D. L. Medlin *et al.*, J. Appl. Phys. **76**, 295 (1994).
[16]D. J. Smith *et al.*, Ultramicroscopy **11**, 263 (1983).
[17]R. M.Wentzcovitch *et al.*, Phys. Rev. B **38**, 6191 (1988).
[18]V. A. Pesin, M. I. Sokhor, and L. I. Fel'dgun, Zh. Fiz. Khim. **53**, 1602 (1979) [Russ. J. Phys. Chem. **53**, 908 (1979)].
[19]S. Nakano and O. Fukunaga, Diamond Relat. Mater. **2**, 1409 (1993).
[20]T. Sato, T. Ishii, and N. Setaka, Commun. Am. Ceram. Soc. **65**, C162 (1982).
[21]T. Sekine and T. Sato, J. Appl. Phys. **74**, 2440 (1993).
[22]A. Onodera *et al.*, J. Mater. Sci. **25**, 4279 (1990).
[23]M. Ueno *et al.*, Phys. Rev. B **45**, 10 226 (1992).
[24]V. F. Britun, A. V. Kurdyumov, and A. Petrusha, J. Mater. Sci. **28**, 6575 (1993).
[25]D. R. McKenzie, W. G. Sainty, and D. Green, Mater. Sci. Forum **54-55**, 193 (1990).
[26]T. Akashi, H. R. Pak, and A. B. Sawaoka, J. Mater. Sci. **21**, 4060 (1986).
[27]D. G. Rickerby *et al.*, Thin Solid Films **209**, 155 (1991).
[28]P. Stadelman, Ultramicroscopy **21**, 131 (1987).

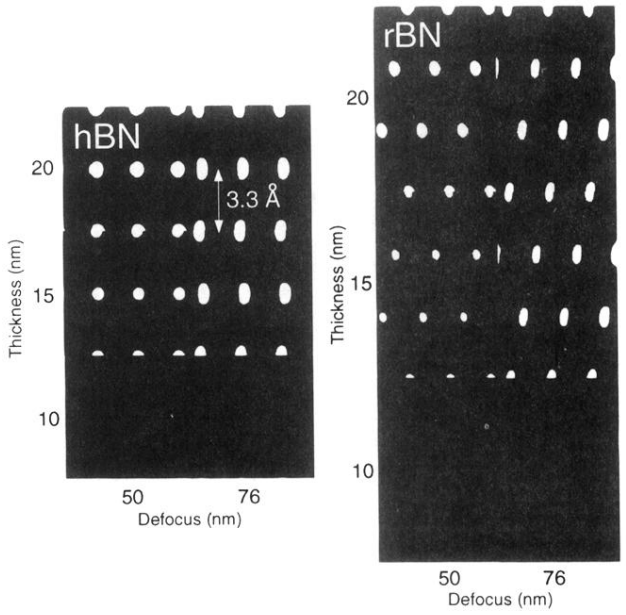

FIG. 2. High-resolution image simulations calculated as a function of thickness and defocus for hBN and rBN oriented along a $\langle 2\bar{1}\,\bar{1}0 \rangle$ direction for the following conditions: electron energy, 400 keV; coefficient of spherical aberration, 1.0 mm; semiconvergence angle, 1.3 mrad; objective aperture diameter, 20 nm^{-1}; and spread of focus, 10 nm. Simulations calculated using the EMS package of electron microscopy routines (Ref. 28).

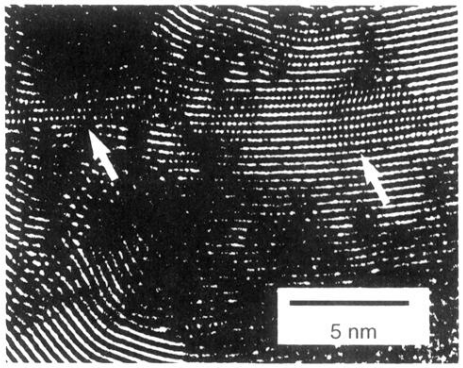

FIG. 3. HRTEM image of turbostratic BN in a film deposited by ion-assisted pulsed-laser deposition. Defocus is 70 nm.

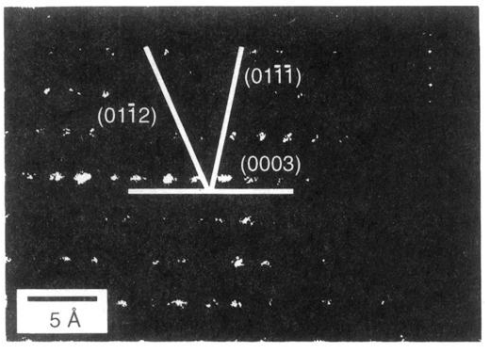

FIG. 4. Enlargement of region indicated by the rightmost arrow in Fig. 3. Angles measured from micrograph are as follows: (0003), (01$\bar{1}\,\bar{1}$), 66±2° (direct), 63±1° (power spectrum) and (0003), (01$\bar{1}$2), 78±1° (direct), 78±1° (power spectrum). Calculated angles for rBN are as follows: (0003), (01$\bar{1}\,\bar{1}$), 66.5° and (0003), (01$\bar{1}$2), 77.8°.